Benefits of Integrated Seismic and Gravity Exploration: An example from Norman Wells, NWT

J. Helen Isaac* and Donald C. Lawton
Fold-Fault Research Project, University of Calgary
2500 University Drive NW, Calgary, AB, T2N 1N4
isaac@geo.ucalgary.ca

ABSTRACT

Interpretation of a gravity survey was integrated with processing of reflection seismic data acquired across the Norman Range, near Norman Wells, NWT. Previous geological mapping had led to the development of three structural models for this area:

(1) A low angle thrust fault in the Upper Cambrian Saline River Formation, causing repetition of dense Palaeozoic dolomites and anhydrites, with no involvement of sub-Saline River sediments.

(2) A high-angle reverse fault thrusting Proterozoic sediments into the core of the Norman Range.

(3) A vertical block fault model with a horst of Proterozoic and basement rocks coring the Norman Range, with no horizontal shortening.

We modelled the theoretical gravity field for each case, constrained by outcrop data, well data and density measurements, and thus determined that the first model is most likely to represent the structure of the Norman Range. This preferred gravity-derived model was then used effectively to assist in the construction of a velocity model for depth migration of the seismic data, which was collected in a difficult data area where carbonates outcrop at surface. Integrated analysis of the two data sets supports a thin-skinned deformational model for the Norman Range.

Introduction

The Norman Range is part of the northern Franklin Mountains lying northeast of Norman Wells (*Fig. 1*). Structural control of the topography of the Norman Range is strongly evident. Dip slopes on the southern flank of the range rise gently from the Mackenzie River to the summit, which is about 800 metres above the valley floor. In contrast, the northern side of the Range is formed by a prominent, linear fault scarp with a northwest to southeast trend, which extends for a distance of over 40 kilometres. *Fig. 1* shows the major physiographic features and structural elements present in the study area.

Geology

Throughout the Franklin Mountains, Proterozoic-aged quartzites, dolomites, limestones and sandstones, possibly several thousand metres thick, overlie the deeper crystalline Precambrian basement. The Norman Range is composed of sandstones, shales, dolomites and evaporates of Palaeozoic age (*Fig. 2*). Beneath the Norman Range, the Proterozoic sequence is unconformably overlain by salt, gypsum and shales of the Upper Cambrian Saline River Formation, which varies in thickness from about 200 to 1000 metres. Cook and Aitken (1973) attributed the variation in thickness to tectonic thickening from compressive deformation during the Laramide Orogeny.

The backbone of the Norman Range is formed by the Franklin Mountain Formation, which is a thick (600 m) sequence of Upper Cambrian and Lower Ordovician dolomites. This formation overlies the Saline River Formation and underlies a succession of Devonian limestones, dolomites and shales. The total thickness of Devonian sediments is approximately 1000 metres. Dolomite and anhydrite of the Lower Devonian Bear Rock Formation grade conformably into fossiliferous thin- and medium-bedded limestone of the Middle Devonian Hume Formation, which in turn is overlain by recessive shales of the Hare Indian Formation. The uppermost mid-Devonian unit is the Ramparts Formation, which is primarily a skeletal-fragmental limestone and is the oil-bearing formation for the Norman Wells field.

The youngest rocks exposed in the Norman Range are Upper Devonian shales and sandstones of the Canol and Imperial Formations. These formations outcrop to the north of the Mackenzie River (*Fig. 2*) but in most places they are covered by a thin veneer of Quaternary glacial sediments. South of the Mackenzie River, Cretaceous sandstones and shales unconformably overlie the Imperial Formation.

Cook and Aitken (1973) proposed that most of the ranges in the Franklin Mountains are underlain by low-angle thrust faults with a detachment zone within the evaporite beds of the Saline River Formation. However, they did note that this structural style is often complicated by enigmatic thrust reversals from one end of a range to the other and that deformation involving older Proterozoic sediments occurs further south in the McConnell Range. Cook and Aitken (1976) later questioned their earlier model and proposed that the observed structures in the Norman Range are also consistent with high-angle reverse faulting involving sub-Saline River strata. Furthermore, Davis and Willot (1978) documented a convincing case for the involvement of Proterozoic sediments in faulting in the Colville Hills, which lie 200 km to the north of the Norman Range. Their interpretation was that deep deformation involved basement faults and they extrapolated their Colville Hills model to include the geometrically similar Franklin Mountains. From this work emerge three possible models for deformation in the Norman Range:

(1) Low-angle thrust faulting with detachment in the Saline River Formation and subsequent horizontal shortening.
(2) High-angle reverse faulting with detachment within the Proterozoic section.

(3) Basement-related block faulting.

Gravity Survey And Reductions

The gravity survey was undertaken to determine whether the Saline River Formation has been tectonically thickened within the core of the Norman Range. It was presumed that any thickening of the evaporites would result in a negative residual Bouguer anomaly across the structure because of the negative density contrast of salt with respect to limestone and dolomite.

A 16-km profile consisting of 123 gravity stations (*Fig. 2*), mostly perpendicular to the strike direction of the Norman Range (approximately 110º), was laid out. The average station interval was 200 m but this was reduced to 50 m in areas of irregular topography on the southern slopes of the Norman Range. All gravity measurements were made with a Worden Master gravity meter and readings were tied in to the Earth Physics gravity station #59777. Base stations were established along the profile and were reoccupied every 1.5 to 2 hours to record instrument and diurnal drift. Twelve stations were reoccupied independently to check repeatability, which was found to be within ±1 $\mu m/s^2$ after correction for drift.

The Bouguer anomalies were calculated using a uniform density of 2.67 x 10 kg/m^3 and a sealevel datum. Terrain corrections to a distance of 22 km from each station were determined using the template method of Hammer (1939). The average terrain correction over all the stations was 20 $\mu m/s^2$, with individual values reaching 50 $\mu m/s^2$ at stations on the higher parts of the Norman Range. The uncertainty in the Bouguer anomaly values is estimated to reach values of ±5 $\mu m/s^2$ for stations south of the summit. North of the escarpment, the terrain corrections are small (generally less than 2 $\mu m/s^2$) and uncertainty in the Bouguer anomalies is caused primarily by the uncertainty in the elevation.

Gravity data interpretation

For data analysis, station positions were projected on to a straight line with an azimuth of 023º (*Fig. 2*). The Bouguer anomalies versus projected distance along this azimuth are plotted in the upper part of Figure 3. The scatter in the data over the Norman Range reflects the increasing uncertainty in the terrain corrections in the summit region.

The calculated regional field was subtracted from the observed Bouguer anomalies to yield residual Bouguer anomalies (right scale of *Fig. 3*), which reflect the density structure within the Norman Range. Tectonic thickening of the Saline River Formation is negated because there is no evidence of a relative negative anomaly over the main part of the range. The negative anomaly at the southern end of the profile is caused by an increasing thickness of lower density shale sequences.

Control for the interpretation of the data was provided by:

(a) Outcrop geology from geological maps (Cook and Aitken, 1976).

(b) Stratigraphic thicknesses and average densities of formations, obtained from wells.

(c) Density measurements from hand specimens. For the Saline River Formation, an evaporite and shale sequence, we assumed a realistic average density of 2.30 x 10^3 kg/m^3.

In addition to these controls, we also made various assumptions to provide constraints on the density structure in the subsurface:

(a) The stratigraphic thicknesses are constant along the section unless altered by the results of gravity modelling.

(b) The formation densities are constant along the section.

(c) The major structures are two-dimensional.

Density models along the section were constrained by the known boundary conditions and these assumptions. The theoretical residual gravity anomaly at each station was evaluated by a two-dimensional gravity modelling computer program for each of the three models. These models and the calculated anomalies are shown in *Fig. 3* and are discussed below.

(1) Low-angle thrust fault (*Fig. 3a*). The observed relative positive gravity anomaly is caused by repetition of dense dolomites and anhydrites of the Franklin Mountain, Hume and Bear Rock formations. A low angle thrust fault is inferred to place this repetition in its correct spatial position relative to the anomaly maximum. Detachment is entirely within the Saline River Formation, which has become tectonically thickened in the southwestern part of the section (stations 100-120) and locally thickened below the summit of the Norman Range (stations 188-196). There is no involvement of sub-Saline River sediments. High-angle reverse faults mapped in the summit region by Cook and Aitken (1975) are considered to be minor secondary faults off the main thrust, which requires at least 9 km of shortening of the post Proterozoic sediment cover.

(2) High-angle reverse fault *(Fig. 3b*). The major structure is a high-angle reverse fault with the core of the Norman Range infilled with Proterozoic sediments, i.e. the deformation involves sub-Saline River strata. Secondary en-echelon reverse faults cause additional minor offsets in the summit region. Total horizontal shortening is only about 3 km. However, for this model to generate the observed relative positive gravity anomaly, the Proterozoic sediments are required to have a density of at least 2.84 x 10^3 kg/m^3 (i.e. a dolomite lithology).

(3) Vertical block fault model (*Fig. 3c*). The Norman Range scarp is caused by a vertical fault with a throw of 1.5 km. There is no horizontal shortening and the structure is entirely caused by block faulting of the Proterozoic and basement rocks. However, as in the Proterozoic detachment model

(*Fig. 3b*), it is necessary to give the Proterozoic sediments the higher density of 2.84 x 10^3 kg/m^3 to match the observed gravity data. If a more reasonable Proterozoic density of 2.67 x 10^3 kg/m^3 is used, there is a poor fit between the computed and observed data.

In all of the final models, the Ramparts Formation has to thicken significantly where it outcrops at the Kee Scarp (stations 124-142) to enable a good fit between the observed and calculated anomalies to be obtained. This may represent a reef to back-reef facies.

Seismic Data Processing

An 8-km seismic line acquired near Norman Wells in 1996 was kindly provided to the study by Murphy Oil. The survey consisted of 336 shots spaced at 32 m, 240 recording channels spaced at 8 m and farthest offsets nominally 960 m. The quality of the data varied greatly, with some shots having considerable noise. In *Fig. 4a* the two shot gathers display different noise trains and the pattern of first breaks show how drastically the near-surface velocity varies along the line. The near-surface velocity model derived by GLI3D refraction statics analysis indicated higher sub-weathering velocities in the western part of the survey and only a thin weathered layer, which is absent at the highest elevations. These high near-surface velocities are interpreted to be caused by outcropping carbonate formations.

The pre-stack data processing included surface wave noise attenuation, predictive deconvolution, trace equalization, radial filtering and *f-k* filtering. The final filtered shot records (*Fig. 4b*) show good reflectivity at shot 50 but the signal/noise ratio of shot 150 is still quite low. We derived stacking velocities by both semblance analysis and constant velocity stacks, applied residual statics and post-stack time migrated the data. The final post-stacked time migrated section (*Fig. 5*), which has had a coherency filter applied, shows a few strong, continuous reflectors but it is hard to interpret the structure. The data are only well imaged on the right part of the line, where a thick sequence dips gently to the west. The gap in the data immediately to the west of this continuous section is a result of a gap in the shooting sequence over the escarpment. Fold is low here and the subsurface not well imaged. We do not see any evidence for steeply dipping or uplifted basal reflectors, as proposed in the structural models of *Figs 3b and 3c*.

The data were imported into GX Technology's Sirius software for velocity analysis and pre-stack depth migration (PSDM). Determination of the velocity model was not easy as the data contain offsets only to 960m. After determination of the best velocity model by the method of flattening offset gathers, we remigrated with a new initial velocity model created using the geometry of the preferred model and velocities estimated by previous PSDM analysis. After several iterations of velocity analysis and PSDM of this velocity model we were able to achieve a better focussed migrated depth section. This velocity model was used to create a synthetic zero-offset time section by finite-difference modelling. The synthetic section was then compared to the processed time section and the velocity model adjusted slightly until the geometries of the major reflectors on both sections were comparable. This revised velocity model was then used to create the latest PSDM section (*Fig. 6a*). This section supports the low-angle thrust fault model (*Fig. 6b*), as it does not provide any evidence for normal or reverse faulting involving an uplifted basement. Further refinements of the velocity model and depth section will be used to modify the low angle thrust fault gravity model and compare the ensuing theoretical gravity data with the observed data.

Discussion And Conclusions

The Saline River detachment model is preferred to either of the two models involving Proterozoic faulting for two reasons:

(a) These two models require an unlikely high density of 2.84×10^3 kg/m^3 for the Proterozoic sediments in order for the observed and modelled gravity profiles to match.

(b) The processed seismic line supports the thin-skinned detachment model because deep reflections (at 2000 m) show no significant structure.

Although Cook and Aitken (1976) preferred the Proterozoic detachment model to the Saline River detachment model because of high-angle short displacement reverse faults observed elsewhere in the northern Franklins, we propose that these structures can indeed be accommodated in the Saline River detachment model. Those faults are considered minor, secondary features associated with flexing of the main thrust sheet (*Fig. 3a*). The Saline River detachment model also indicates that the Ramparts Formation (the main reservoir rock) should extend below the Norman Range in the lower thrust sheet.

The study illustrates how a gravity-derived model can be used effectively to assist in the construction of a seismic velocity model for depth migration of seismic data collected in a difficult data area where carbonates outcrop at surface. Integrated analysis of the two data sets supports a thin-skinned deformational model for the Norman Range with a décollement in Upper Cambrian salt strata of the Saline River Formation.

Acknowledgements

We thank Dr. D. Cook and Mr. D. Pugh of the Geological Survey of Canada. Mr. B. McLean assisted in the gravity data collection. We thank Murphy Oil for providing the seismic data. We also acknowledge the financial support for this work by sponsors of the Fold-Fault Research Project and the donation of software by Landmark Graphics, GX Technology and Hampson-Russell.

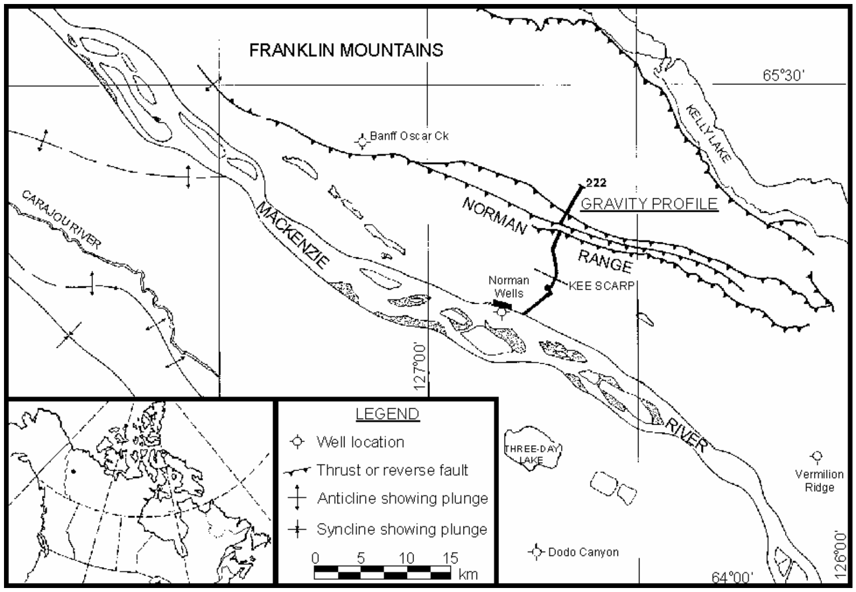

Fig. 1. Index map.

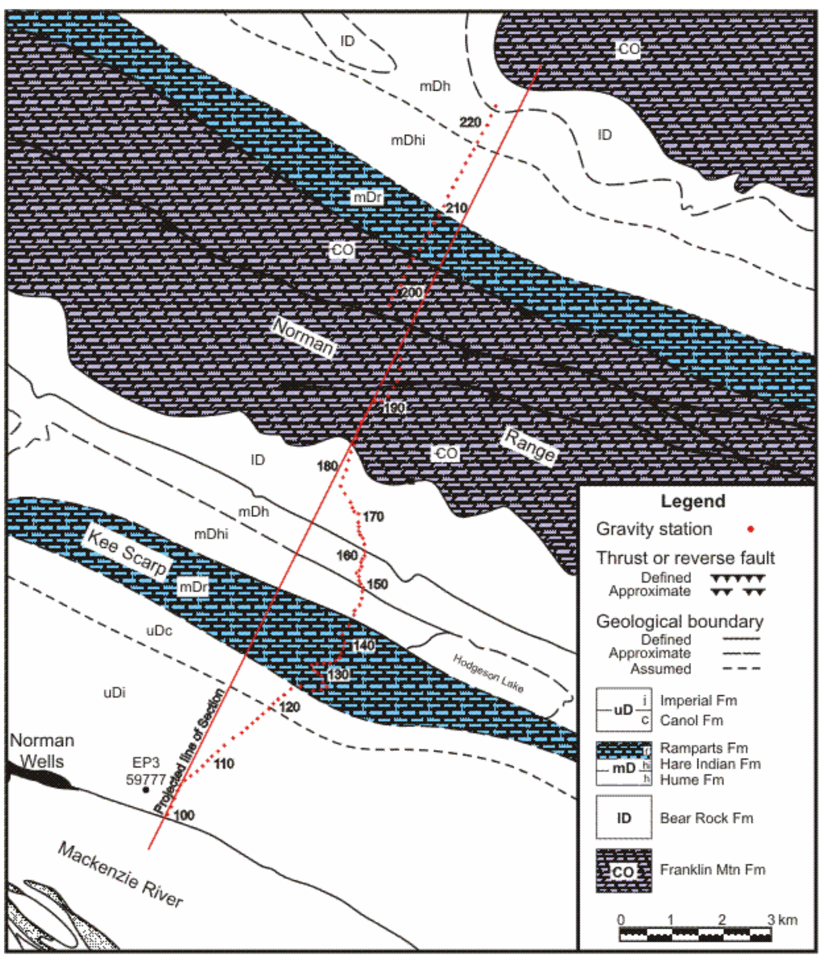

Fig. 2. Detailed geology map of the area encompassing the gravity profile.

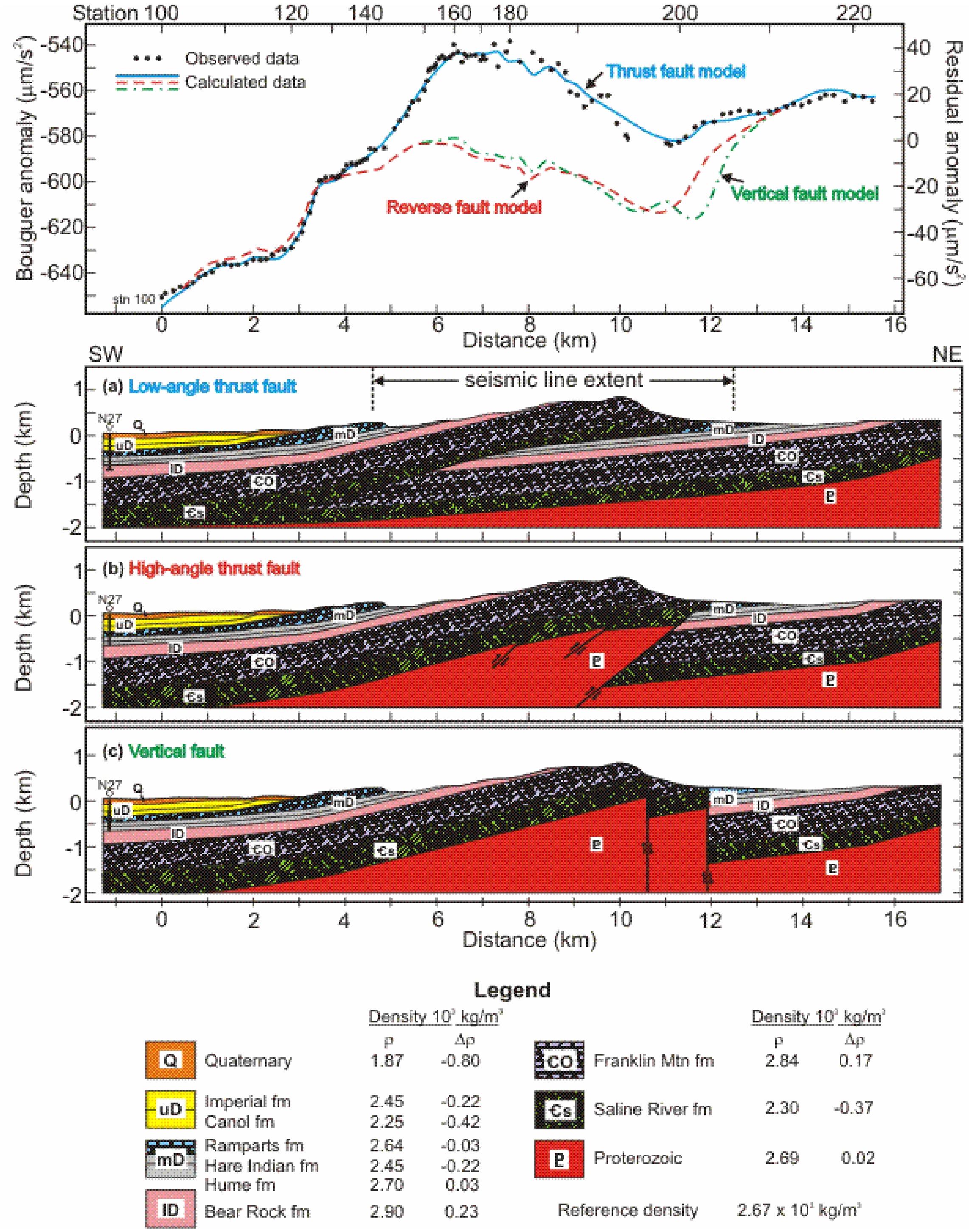

Fig. 3. Bouguer anomalies and various structural interpretations of the anomalies. The low-angle thrust fault model (3a) is preferred.

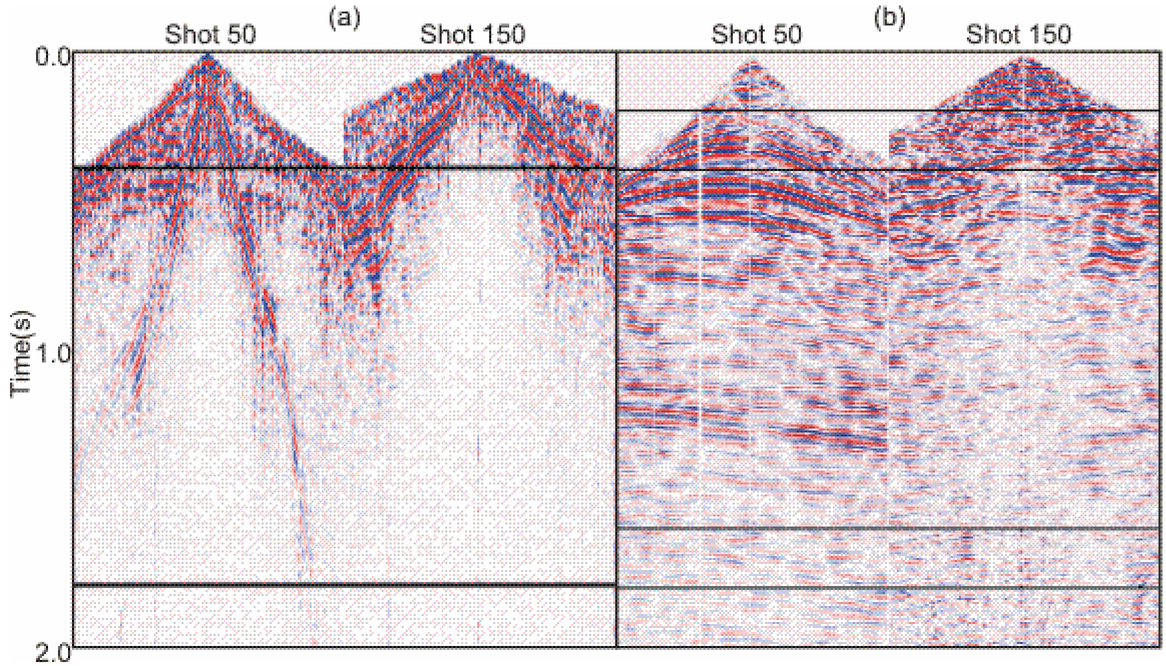

Fig. 4. (a) Two shot gathers from the Norman Wells survey. The pattern of first breaks shows how the near-surface velocity varies drastically along the line. Also, different noise patterns are apparent. (b) The final processed gathers.

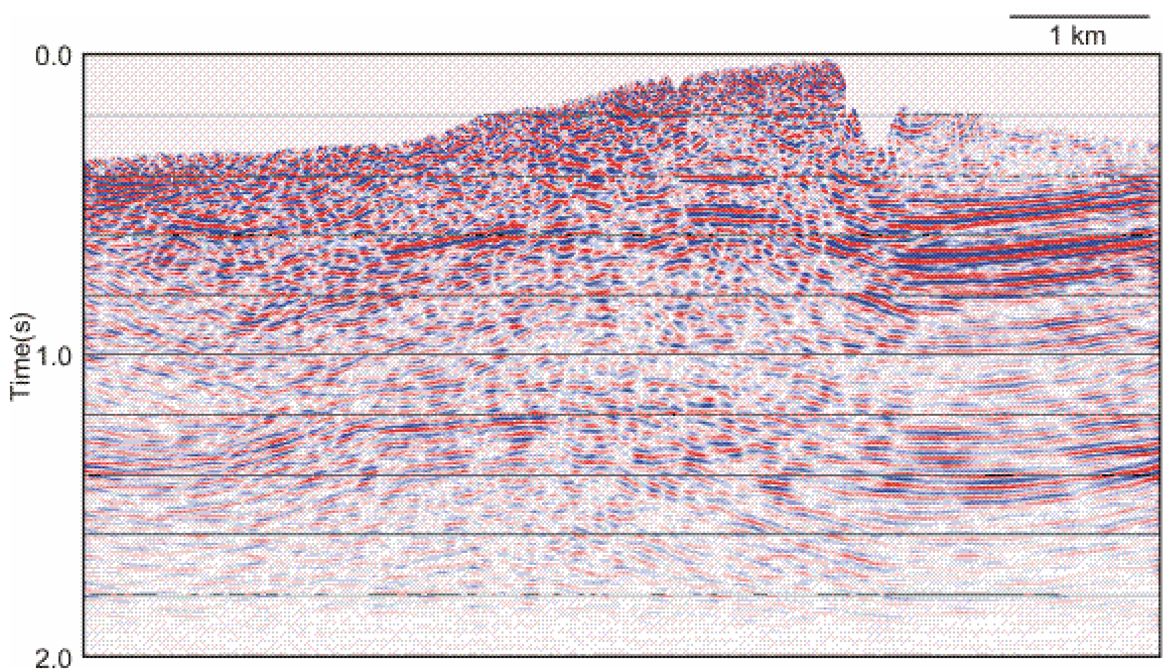

Fig. 5. Post-stack time migrated section.

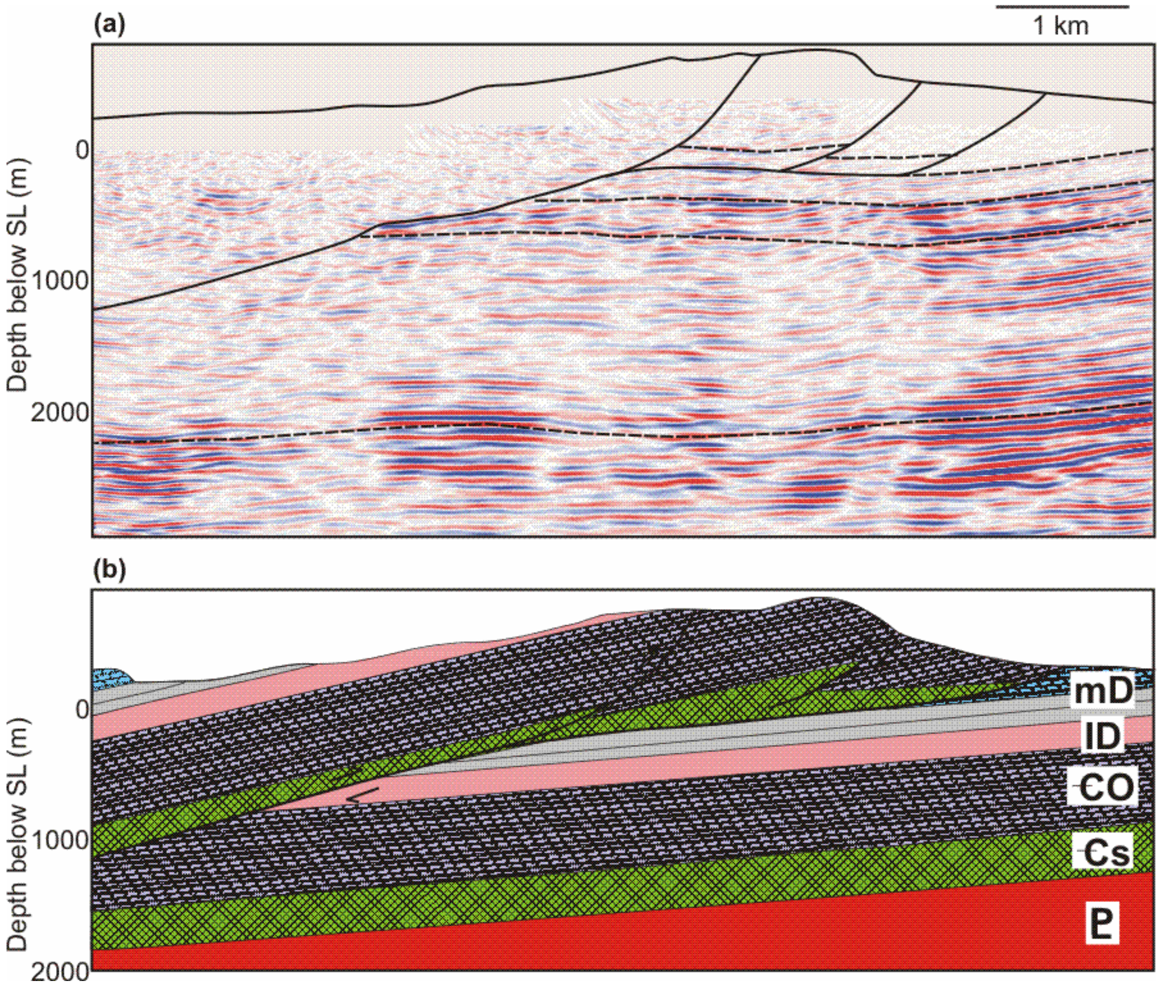

Fig. 6. (a) The final pre-stack depth migrated seismic data with the major faults marked by solid lines and the major lithologic boundaries by dashed lines. (b) The preferred gravity model displayed at the same scale as the seismic data.

References

Cook, D. G. and Aitken, J. D., 1973, Tectonics of the northern Franklin Mountains and Colville Hills, District of Mackenzie, Canada, in Arctic Geology: Am. Assoc. Petr. Geol., Mem. 19, 13-22.

Cook, D. G. and Aitken, J. D., 1975, 1:250,000 geological map of the Norman Wells region: Department of Energy, Mines and Resources.

Cook, D. G. and Aitken, J. D., 1976, Two cross-sections across selected Franklin Mountain structures and their implications for hydrocarbon exploration: Geological Survey of Canada, Paper 76-1B.

Davis, J. W. and Willott, R., 1978, Structural geology of the Colville Hills: Bull. of Canadian Pet. Geol., 26, no. 1, 105-122.

Hammer, S., 1939, Terrain corrections for gravimeter stations: Geophysics, 4, 1412-1426.